Separation and Purification Technology 186 (2017) 182–187

Contents lists available at ScienceDirect

Separation and Purification Technology

journal homepage: www.elsevier.com/locate/seppur

Analysis of energy costs for catalytic ozone membrane filtration

Xiaoyu Wang, Simon H. Davies, Susan J. Masten *

Department of Civil and Environmental Engineering, Michigan State University, East Lansing, MI 48824, USA

ARTICLE INFO

Article history:
Received 12 December 2016
Received in revised form 24 March 2017
Accepted 19 April 2017
Available online 3 June 2017

Keywords:
Membrane fouling
Ozonation
Ceramic membrane
Catalytic membrane
Water treatment
Energy cost analysis

ABSTRACT

Membrane fouling can be reduced through shear stress generated by cross-flow at the membrane surface. Previous work has shown that presence of ozone can reduce membrane fouling. In this work, the effect of ozonation and cross-flow on both membrane fouling on ceramic membranes and the energy cost for the process was studied. The effect of ozone dosage on membrane fouling was studied in both cross-flow and dead-end configurations. The performance of a manganese oxide coated membrane was compared with that of uncoated titanium oxide membrane. Membrane fouling decreased with increasing ozone dosages in the manganese oxide coated catalytic membrane, although increasing the dosage beyond 10–15 μg/s yielded limited improvement. The most energy-efficient mode of operation was found to be dead-end filtration using a manganese oxide coated membrane and a 10 μg/s ozone injection rate.

1. Introduction

Ultrafiltration (UF) membrane filtration can effectively remove suspended particles, colloids, bacteria, viruses and significant fraction of natural organic matter (NOM) from feed water [1]. There are a number of advantages of UF membrane treatment over conventional water treatment technologies, including reduced sludge production [2], smaller footprint [3], and the physical exclusion of microorganisms from the product water. However, membrane fouling continues to be one of the main factors that limit the application and increase the operational costs of membrane technologies [4]. Fouling results in a decrease in the production rate of purified water and a concomitant increase in the requisite transmembrane pressure [5].

In water treatment, NOM is the predominant cause of UF membrane fouling [6–9]. The use of ozone in combination with membrane filtration has been reported to reduce membrane fouling [10–14]. Ozone, a powerful oxidant, is reactive with NOM [15]. Pre-ozonation can also reduce formation of trihalomethanes (THMs) during subsequent chlorination [16].

Ceramic membranes are chemically stable, have longer lifetimes than polymeric membranes, and they can be used in conjunction with ozonation without degradation of the membrane [17,18]. Moreover, the surface properties of ceramic membranes may be altered to improve membrane performance. Metal oxides, such as titania [10,11], iron oxide [11], and manganese oxide [11,19,20], can act as catalysts for the degradation of ozone and the formation of hydroxyl radicals. These catalytic reactions are assumed to occur at the metal oxide surface. Kim et al. [12] studied the performance of nanoparticle-enhanced membranes and concluded fouling was dependent upon the physicochemical aspects of nanoparticles, such as particle size, hydrophilicity, and surface charge. Byun [11] reported that when used with ozone the performance of the manganese oxide coated membrane was superior to that of Ti and Fe oxide membranes in terms of fouling mitigation and the reduction of TOC in the permeate. In addition, the coating of the membranes with manganese oxide nanoparticles significantly reduced the concentrations of THM and haloacetic acids (HAA) precursors found in the permeate [19]. Szymanska et al. [13] and Zouboulis et al. [21] showed that with hybrid ozonation ceramic membrane microfiltration, mitigation of membrane fouling was well controlled. Wei et al. [22,23] demonstrated that pre-ozonation mitigated fouling on a UF membrane that was caused by soluble extracellular organic matters that had been released from *Microcystis aeruginosa.* They found that ozone reacted with the cake and gel layers and prevented membrane pore blocking.

The objective of this study was to analyze the energy costs for membrane filtration, in the presence of ozone, using either a manganese oxide coated ceramic membrane or titania oxide coated membrane (virgin membrane). Studies were conducted to determine the optimum ozone dosage and hydrodynamic conditions for this hybrid membrane system. The energy costs for both ozone generation and pumping were evaluated to determine the operating conditions for which the energy costs were minimized.

* Corresponding author.
E-mail address: masten@egr.msu.edu (S.J. Masten).

http://dx.doi.org/10.1016/j.seppur.2017.04.055
1383-5866/

2. Experimental methods

2.1. Feed water

The source water was obtained from Lake Lansing (Haslett, Michigan), a borderline eutrophic lake. The water was stored in the dark at 4 °C until use. Water samples were pre-filtered through a 0.5-μm ceramic cartridge micro-filter (Doulton USA, Southfield, MI) to remove larger particles. After filtration, the average TOC concentration in the test water was 10 ± 1 mg C/L. Before commencing each experiment, the temperature of the feed water was adjusted to room temperature (20 ± 3 °C).

2.2. Membrane module

The nominal molecular weight cut-off of the virgin membrane (Inside CeRAM, TAMI North America, Saint - Laurent, Quebec, Canada) was 5 KDa. The seven-channel membrane had a total filtering surface area of 131.9 cm^2, an active length of 25 cm, and an external diameter of 10 mm. The grain size within the support layer and the filtration layer of the virgin membrane varied between 132 nm and 296 nm and between 1.05 and 6.64 nm, respectively [11]. The clean water permeability of the coated membrane was 80 ± 2 L/m^2 h.

The virgin membrane was coated with manganese oxide according to the procedure described by Corneal et al. [20]. In this study, the performance of a membrane coated twenty times manganese oxide nanoparticles was examined, as higher permeate fluxes were obtained with membrane coated twenty times coated than with those coated thirty or forty times. Byun et al. [11] found the Mn oxide coating to be crystalline Mn_2O_3, and that for the membrane that was coated 20 times, the thickness of coating ranged from 14 to 54 nm. With the manganese oxide coated membranes, the lower operating pressure was used because the permeability of the manganese oxide coated membrane was higher than that of the uncoated membrane, as sintering at 500 °C leads to coarsening of the grains within the filtration layer [19].

2.3. Ozone contactor

A schematic for the ozone contactor is shown in Fig. 1. The water in the contactor was maintained at a constant level using a conductivity water level sensor connected to a programmable logic relay (SG2 PLR, B&B Electronics, IL), which opened or closed a solenoid valve (6013, Bürkert, Germany) to regulate water flow from the sample reservoir to the contactor. Ozone was generated from pure, dry oxygen (99.999%) using a corona discharge ozone generator (Absolute Ozone®, Absolute System Inc., Edmonton, AB, CA). An ozone monitor (Model 450H, Teledyne Technologies Inc., San Diego, CA) was used to measure ozone concentration. The flow rate of ozone gas was controlled at 10 mL/min by a rotameter (Cole-Parmer Inc., Vernon Hills, IL) installed between the ozone monitor and the membrane module. The ozone transfer efficiency in the contactor was determined before each experiment, by measuring the difference in the influent and effluent gaseous ozone concentrations and multiplying that difference by the gas flow rate.

2.4. Hybrid ozonation – filtration setup

The schematic of the ozone injection system is shown in Fig. 1. Nitrogen gas (99%, Airgas) was used for pressurizing feed tanks. The membrane module housing (TAMI North America, St. Laurent, Québec, Canada) was made of stainless steel. Both dead-end filtration and cross-flow filtration were performed at volumetric flow rate through the membrane of 18 ± 1.5 mL/min. This corresponds to a flux of 81.2 ± 2.8 L/m^2 h, which is typical of that used in full-scale water treatment. The flux was maintained using a peristaltic pump (Eldex®, Eldex Laboratories, Inc., Napa, CA). A recirculation pump (Materflex®, Cole Parmer Inc., Vernon Hills, IL) used when operating the system in cross-flow mode to obtain the constant cross-flow velocity of 0.5 ± 0.1 m/s. The transmembrane pressure (TMP) was recorded by a multifunctional sensor (L Series, Alicat Scientific, Tuscon, AZ) every 60 s. Temperature and atmosphere pressure were also monitored every 60 s by the multifunctional sensor. The permeate flux was measured using an electronic balance (Adventure Pro Analytical Balance, Ohaus Corp., Pine Brook, NJ) every 60 s. The transmembrane pressure (TMP, bar) and permeate flux (J, L/m^2 h) were recorded by Flow Vision SC (Alicat Scientific, Tucson, AZ) data acquisition software.

Experiments were conducted at ozone dosage injection rates of 5, 10, 15, and 20 μg/s. Control experiments were conducted to measure membrane flux without gas injection. The range of ozone dosages was selected based on prior work, which indicated that ozone dosages greater than 20 μg/s resulted in little enhancement

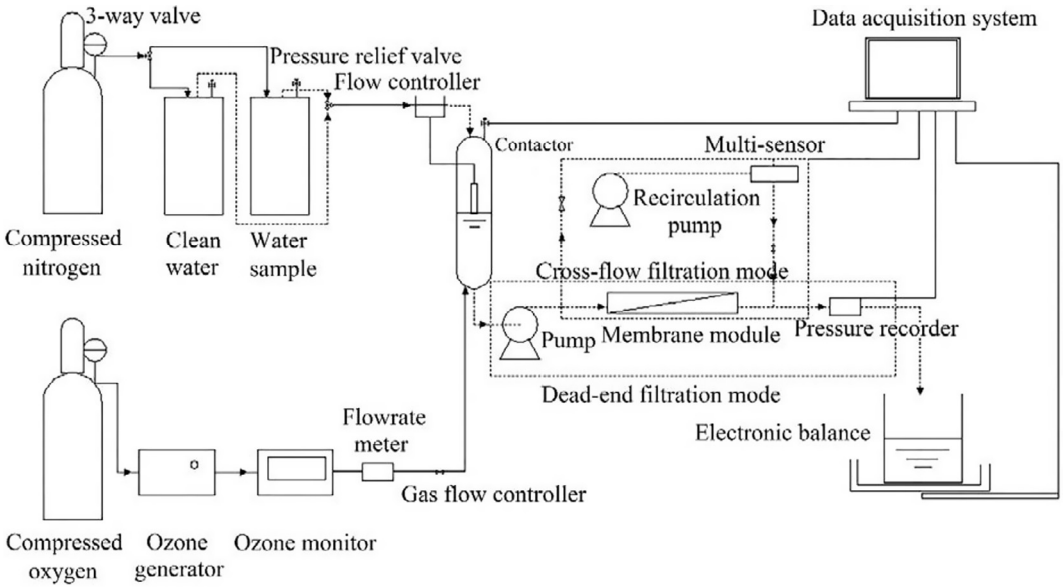

Fig. 1. Schematic of the ozonation-membrane filtration system.

in the permeate flux and reduction in membrane fouling [14,21,24]. Experiments were halted when the permeability of the membrane decreased to approximately 40% of the initial permeability.

After each experiment, the fouled membranes were cleaned using deionized water and 20 μg/s gaseous ozone for 2–4 h until the initial clean water flux was restored. Before each filtration experiment, the initial flux was measured to ensure that the permeability of the membrane was within (98 ± 2)% of its initial value [11]. After cleaning the initial TMP for the system varied between 1.2 and 1.5 bar.

2.5. Data analysis

2.5.1. Permeability and resistance fouling

The permeability, L_p, was calculated as shown in Equation (1):

$$L_p = \frac{J}{TMP} \tag{1}$$

where L_p is given in units of L/(m^2 h·bar). The greater the permeability, the higher the efficiency of the membrane.

The total resistance across the membrane was calculated from the TMP and flux data using Darcy's Law:

$$R_t = \frac{\mathrm{TMP}}{\mu J} \tag{2}$$

$$R_t = R_m + R_c \tag{3}$$

where μ is the viscosity of water at 22 ± 2 °C (0.89×10^{-3} N s/m^2). The total resistance, R_t, is the sum of the intrinsic resistance of the membrane, R_m, and the resistance due to the material deposited on the membrane surface, R_c. R_t was calculated from the final TMP and flux.

2.5.2. Calculation of energy consumption

2.5.2.1. Energy consumed to pressurize feed water. The power necessary to pressurize the feed water was determined by Eq. (4) [25]:

$$P_h = \frac{q \cdot \rho \cdot g \cdot h}{\eta} = \frac{q \cdot TMP}{\eta} \tag{4}$$

where q (m^3/s) is the average flow rate of the membrane module during the operational period and is calculated by $q = \pi d^2/4 \times v$, v is the velocity of the water in filtration system; ρ (kg/m^3) is the density of feed water at room temperature; g (9.81 m/s^2) is gravitational acceleration of the earth; h is the water head (m), TMP (bar) is the transmembrane pressure across membrane module, and is calculated using the equation TMP = ρgh, η is the efficiency of the pressurizing pump which was assumed to be 75%. The power (P_h) is reported in units of kW.

2.5.2.2. Energy consumed by recirculation pump. The power required to recirculate water through the system was determined by Eq. (5) [25]:

$$P_r = \frac{q \cdot \rho \cdot g \cdot \Sigma h_r}{\eta'} = \frac{q \cdot \Sigma \Delta P}{\eta'} \tag{5}$$

in which P_r is in kW; the total water head ($\Sigma h_r = \Sigma \Delta P/\rho g$) of the recirculation system was determined from pressure drop (ΔP) across the tubing and membrane module, η′ is the efficiency of the pressurization pump, which was determined to be 70% based on the pump curve.

The pressure drop in the system was calculated using Darcy–Weisbach equation:

$$\Delta P = \frac{f \rho v^2 L}{2d} \tag{6}$$

Table 1
Backwash process operation parameters.

Criteria	Parameters
Duration	2–4 h, take 3 h as average
Fouled membrane TMP	2.2–2.6 bar for high ozone injection rate (> 10 μg/s); 3.6–4.0 bar for no ozone injection or 5 μg/s ozonation
Cleaned membrane TMP	1.2–1.5 bar
Average membrane TMP during backwash process	Approximately 1.9 bar for high ozone injection rate (>10 μg/s); 2.58 bar for no ozone injection or 5 μg/s ozonation
Feed water flow rate	~18 mL/min
Ozone injection rate	20 μg/s

$$fR_e = 64 \tag{7}$$

$$R_e = \frac{dv\rho}{\mu} \tag{8}$$

where ν is cross-flow velocity (0.5 ± 0.1 m/s during experiment), f is the Darcy friction factor, d (m) is the hydraulic diameter of the pipe/membrane channels, ρ (kg/m^3) is the density of feed water under room temperature, L (m) is the length of different tubing sections. For the recirculation cycle, ΔP was calculated separately across the different sections of tubing, valves, and membrane channel using an online pressure drop calculator (Pressure Drop Online-Calculator. Software-Factory Norbert Schmitz.).

2.5.2.3. Energy consumption during ozone generation in backwash and operation cycles. Based on product data sheet ozone generator (Primozone Production AB.), Ozone Generators parameters (Lenntech BV.) and published literature [26], approximately 10 kW h energy is consumed to produce 1 kg ozone from. The ozone transfer efficiency in the system was determined to be 95% based on the analysis of dissolved ozone concentrations and the ozone concentration in the gas phase before and after the contactor.

The operational period was determined by the filter run time between backwashing. The filters were backwashed when transmembrane pressures reached 2.5 ± 0.1 bar (>10 μg O_3/s) or 3.8 ± 0.2 bar (<5 μg O_3/s). Gaseous ozone was used for membrane backwash cleaning. The operational parameters for the backwashing are shown in Table 1. The energy needed for backwashing, including that required for pressurization during backwash process and that for generating ozone. The energy consumed during operation was W = P × T, in which W is in kW h, P (kW) is the power required to pressurize the feed water or recirculate water, and T is the operation time.

3. Result and discussion

3.1. Comparison of permeate flux and resistance fouling

Fig. 2 displays the effect of ozone dosage on permeate flux during catalytic membrane filtration when a manganese oxide coated membrane was employed using dead-end operation mode. As shown in this figure, irrespective of ozone dosage, the permeability initially declined rapidly during first 30 min. In this stage, the fouling cake begins to form at membrane surface. This stage was followed by one in which the permeability decreased at a much slower pace. At an ozone dosing rate of 20 μg/s the permeability was eventually nearly constant. When the permeability reached steady state condition, the rate of formation of the fouling cake due to deposition of natural organic matter on the surface of the membrane is presumed to be similar to the rate of reaction of the accumulated foulants with ozone and OH radicals formed as a result of the catalytic degradation of ozone by manganese oxide

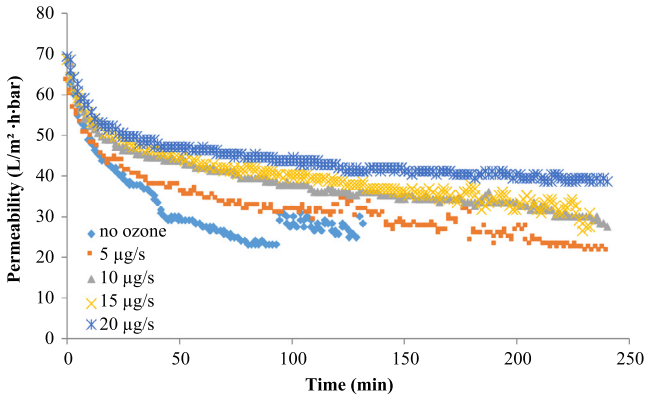

Fig. 2. Effect of ozone dosage on permeability using manganese oxide coated catalytic membrane filtration – dead-end operation mode (Conditions: permeability in L/m^2 h bar, Feed TOC = 12.1 mg/L, temperature = 22 ± 2 °C).

[19]. Increasing the ozone dosing rate improved the performance of the system as catalytic degradation of the filter cake became increasingly favored over formation of the filter cake.

Fig. 3 shows the effect of ozone dosage on permeate flux during cross – flow operation. While the observed permeability trends for cross-flow and dead-end operational modes are similar, the permeability fluctuated more during cross-flow operation than in dead-end operation. As was the case with dead-end filtration, increasing the ozone dosage resulted in less fouling. In the absence of ozone injection and with ozone injection at dosages of 5–10 µg/s, the permeability values after 240 min were greater in cross-flow mode than that in dead-end mode. Under these conditions shear created by the recirculation of the retentate appears to disrupt fouling cake formation. However, at higher (15 and 20 µg/s) ozone dosages the permeabilities observed during operation were similar in cross-flow and dead-end filtration. This suggests that the reaction of ozone and foulants affects the foulants in such a way that the fouling cake less easily dislodged from the membrane surface.

The permeability of the virgin titanium oxide coated catalytic membrane during operation of membrane filtration in both dead–end and cross–flow filtration mode is shown in Fig. 4. The trends were similar to that observed with the manganese oxide coated membrane, as the extent of fouling decreased with increasing ozone dosage. In the absence of ozone, the extent of fouling was greater on the virgin titania membrane than on the coated membrane. This is likely the result of the electrostatic characteristic of the membrane surface. The point of zero charge of manganese oxide (pH_{zpc} = 2.8–4.5 [27]) is lower than that of titania

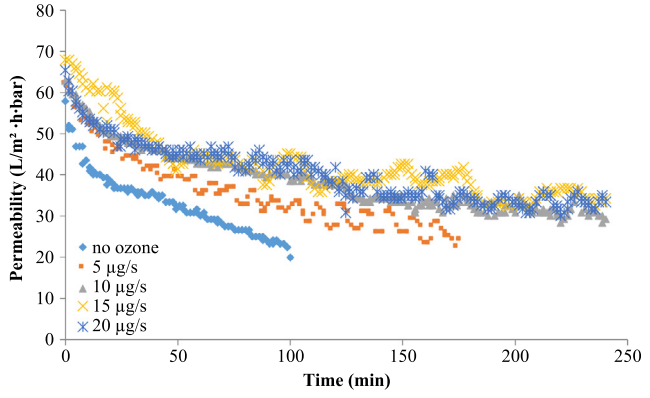

Fig. 3. Effect of ozone dosage on permeate flux during manganese oxide coated catalytic membrane filtration– crossflow operation mode (Conditions: permeability in L/m^2 h bar, Feed TOC = 12.1 mg/L, cross flow velocity = 0.5 ± 0.1 m/s temperature = 22 ± 2 °C).

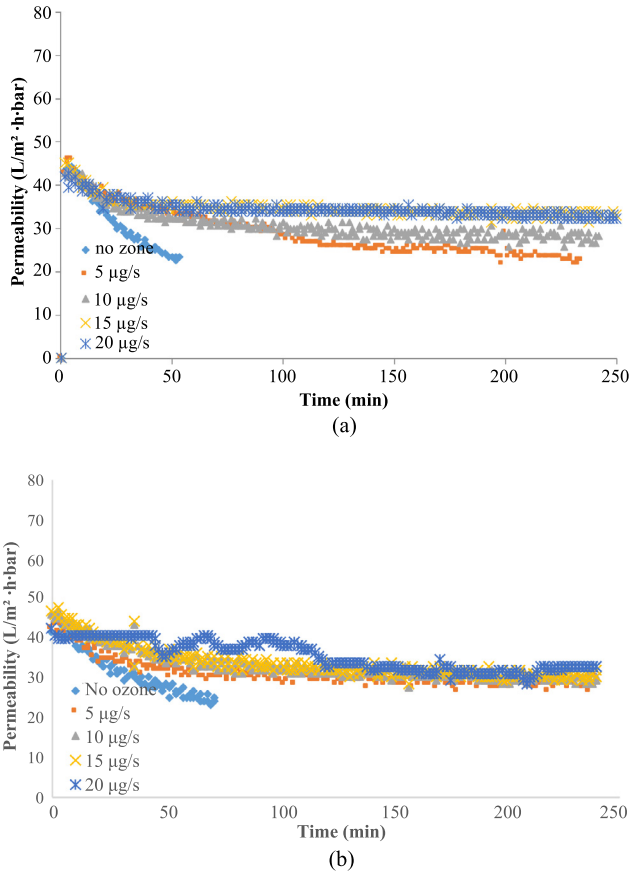

Fig. 4. Effect of ozone dosage on permeability during titania oxide coated catalytic membrane filtration – (a) dead-end operation mode and (b) crossflow operation mode (Conditions: permeability in L/m^2 h bar, Feed TOC = 12.1 mg/L, cross flow velocity = 0.5 ± 0.1 m/s temperature = 22 ± 2 °C).

oxide (pH_{zpc} = 4.1–6.2 [10]). As the pH of the treated water is ~8, the hydroxyl groups on the Mn oxide surface would be fully deprotonated. The surface hydroxyl groups on the TiO_2 surface are not completely deprotonated; thus the manganese oxide surface is likely to have higher charge density and the repulsive forces in the Mn oxide membrane system between the negatively charged components of the NOM and the oxide are probably higher than that observed with the titania oxide membrane. With higher repulsive electrostatic forces, the deposition of organics would be reduced, and with that, the degree of membrane fouling would also be diminished.

The effect of ozone dosage and mode of operation on fouling resistance is shown in Fig. 5. The fouling resistance was determined at 80 min (steady state) for manganese oxide coated catalytic membrane filtration and at 120 min for titania oxide coated catalytic membrane filtration, since as mentioned early, it took longer for steady state conditions to be achieved with the titania oxide coated catalytic membrane filtration. As Fig. 5 shows, the fouling resistance decreased with increasing ozone dosage for both operational modes and membrane types. Recirculation was not as effective as ozonation at reducing fouling resistance. Under identical operational conditions, the resistance of the manganese oxide coated membrane was less than that of the titania oxide coated membrane.

3.2. Energy and economic analysis of membrane systems for design applications

As overall resistance of the manganese oxide membrane, and the operational cost would be less with this membrane under same

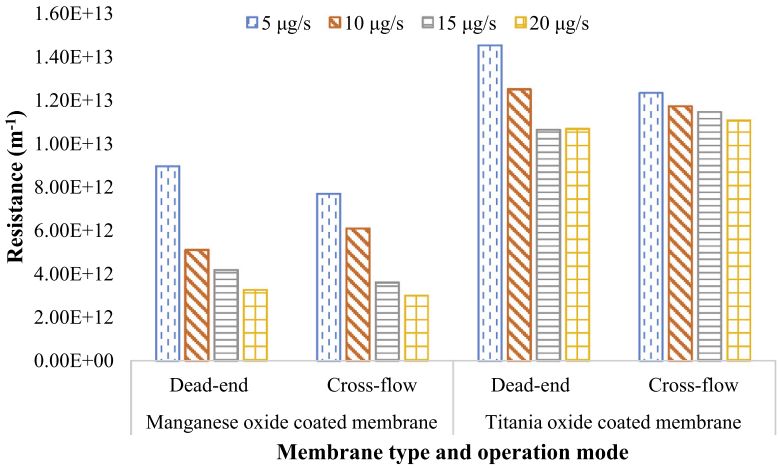

Fig. 5. Effect of ozone dosage on fouling resistance in manganese oxide coated and titania oxide coated catalytic membrane filtration system.

Table 2
Energy consumption for Mn oxide coated membrane filtration with different ozone dosing rates and operation modes with one membrane module.

Operation mode	Ozone dosage (μg/s)	Operation period during 1 cycle (min)	Water filtered during 1 cycle (L)	Energy consumed during operation				Approximate energy needed for 1 cycle backwash cycle (kW h)	Time required to treat 1000 L of water (h)	Numbers of operation periods	Total energy consumed (kW h)
				Energy consumed in pressurization (kW h)	Energy consumed in ozonation (kW h)	Energy consumed in recirculation (kW h)	Total energy consumed during operation (kW h)				
Dead-end	0	93.0	1.563	1.453×10^{-4}	0	0	1.453×10^{-4}	2.583×10^{-3}	1023.7	640	1.75
	5	98.0	1.839	1.728×10^{-4}	3.158×10^{-4}		4.886×10^{-4}		915.6	544	1.67
	10	255.0	4.638	3.530×10^{-4}	1.629×10^{-3}		1.982×10^{-3}	2.502×10^{-3}	927.2	216	0.97
	15	233.0	4.659	4.054×10^{-4}	2.236×10^{-3}		2.641×10^{-3}		844.2	215	1.10
	20	241.0	4.721	3.592×10^{-4}	3.082×10^{-3}		3.441×10^{-3}		861.3	212	1.26
Cross-flow	0	82.0	1.535	1.594×10^{-4}	0	7.291×10^{-5}	2.323×10^{-4}	2.583×10^{-3}	923.0	652	1.83
	5	175.0	3.541	3.585×10^{-4}	5.526×10^{-4}	1.556×10^{-4}	1.067×10^{-3}		837.8	282	1.03
	10	222.0	4.294	3.679×10^{-4}	1.402×10^{-3}	1.974×10^{-4}	1.967×10^{-3}	2.502×10^{-3}	873.3	233	1.04
	15	250.0	4.238	2.952×10^{-4}	2.368×10^{-3}	2.223×10^{-4}	2.886×10^{-3}		995.0	236	1.27
	20	240.0	4.887	4.066×10^{-4}	3.032×10^{-3}	2.134×10^{-4}	3.652×10^{-3}		828.7	205	1.26

ozone dosage and operation mode compared to the virgin titania membrane. Using experimental results for the coated membrane the energy necessary to filter 1000 l of water was calculated (see Section 2.5 and Table 2). The energy costs include energy consumption for pumping water across the membrane, ozone generation, and recirculating through the system. It also includes minor losses through the system. As shown in Fig. 6 for the manganese oxide coated membrane the optimal ozone dosing rate is 10 μg/s for dead end operation and for cross-flow mode it is 5–10 μg/s. At these dosing rates the energy consumed is similar for dead-end and crossflow systems. Dead-end operation is simpler and does not require a recirculation pump thus mode of operation is more desirable. Thus, under the conditions studied for Lake Lansing water, dead-end catalytic membrane filtration using the man-

Fig. 6. Energy consumed during the treatment of in 1000 l of water (including backwash cycles).

ganese oxide coated membrane at an ozone dosage of 10 μg/s was determined to be the most efficient operational mode.

Calculations for energy consumption for the hybrid-ozonation filtration system are given in Section 2.5 data analysis, and results are shown in Table 2. The energy needed to filter 1000 l of water was estimated assuming there was no deterioration in performance over an extended period of time. Based on these calculations the minimum amount of energy required to filter this volume of Lake Lansing water is 0.97kWh.

4. Conclusion

The energy costs for operation of catalytic membrane filtration were calculated. Membrane fouling was effectively controlled using catalytic membrane filtration. For the manganese oxide coated membrane, membrane fouling was effectively controlled at ozone dosages of 10 μg/s or greater. With the virgin membrane, an ozone dosage of at least 15 μg/s was necessary to control membrane fouling. The overall resistance of the manganese oxide membrane was less with manganese oxide coated membrane under same ozone dosage and operation mode compared to that observed for the virgin titania membrane. Using the flux data obtained, it was determined that for the water studied the most energy-efficient operational mode is 10 μg/s ozone dosage, dead-end operation, with the manganese oxide coated membrane. Future work will include a life-cycle assessment (LCA) to evaluate the environmental impacts of membrane filtration, and compare this technology to other water treatment processes, to determine whether this technology is more energy efficient than conventional processes for treating water.

Acknowledgements

This study was supported by the Department of Civil and Environmental Engineering, Michigan State University, and American Water Works Association, Michigan Section. The authors are grateful for the comments from the reviewers of this manuscript.

Appendix A. Supplementary material

Supplementary data associated with this article can be found, in the online version, at http://dx.doi.org/10.1016/j.seppur.2017.04.055.

References

[1] Maryna Peter-Varbanets et al., Mechanisms of membrane fouling during ultra-low pressure ultrafiltration, J. Membr. Sci. 377 (1-2) (2011) 42–53, http://dx.doi.org/10.1016/j.memsci.2011.03.029.
[2] Christopher T. Cleveland, Big advantages in membrane filtration, Am. Water Works Assoc. J. 91 (6) (1999) 10.
[3] R.D. Reardon, Membrane treatment of secondary effluent for subsequent use, Water Intell. Online 6 (2007), http://dx.doi.org/10.2166/9781843397595.
[4] Seyedeh Laleh Dashtban Kenari, Benoit Barbeau, Understanding ultrafiltration fouling of ceramic and polymeric membranes caused by oxidized iron and manganese in water treatment, J. Membr. Sci. 516 (2016) 1–12, http://dx.doi.org/10.1016/j.memsci.2016.06.003.
[5] Haiou Huang, Microfiltration membrane fouling in water treatment, Impact of Chemical Attachments, 2007, Dissertation.
[6] Steven Van Geluwe, Leen Braeken, der Bruggen Van, Ozone oxidation for the alleviation of membrane fouling by natural organic matter: a review, Water Res. 45 (12) (2011) 3551–3570, http://dx.doi.org/10.1016/j.watres.2011.04.016.
[7] Hyun-Chul Kim, Brian A. Dempsey, Membrane fouling due to alginate, SMP, EfOM, humic acid, and NOM, J. Membr. Sci. 428 (2013) 190–197, http://dx.doi.org/10.1016/j.memsci.2012.11.004.
[8] Jaeweon Cho, Amy Gary, John Pellegrino, Membrane filtration of natural organic matter: comparison of flux decline, NOM rejection, and foulants during filtration with three UF membranes, Desalination 127 (3) (2000) 283–298, http://dx.doi.org/10.1016/S0011-9164(00)00017-5.
[9] Kerry J. Howe, Mark M. Clark, Fouling of microfiltration and ultrafiltration membranes by natural waters, Environ. Sci. Technol. 36 (16) (2002) 3571–3576, http://dx.doi.org/10.1021/es025587r.
[10] Jeonghwan Kim et al., Interactions of aqueous NOM with nanoscale TiO_2: Implications for ceramic membrane filtration-ozonation hybrid process, Environ. Sci. Technol. 43 (14) (2009) 5488–5494, http://dx.doi.org/10.1021/es900342q.
[11] S. Byun et al., Mn oxide coated catalytic membranes for a hybrid ozonation–membrane filtration: comparison of Ti, Fe and Mn oxide coated membranes for water quality, Water Res. 45 (1) (2011) 163–170, http://dx.doi.org/10.1016/j.watres.2010.08.031.
[12] Jeonghwan Kim, Bart Van der Bruggen, The use of nanoparticles in polymeric and ceramic membrane structures: review of manufacturing procedures and performance improvement for water treatment, Environ. Pollut. 158 (7) (2010) 2335–2349, http://dx.doi.org/10.1016/j.envpol.2010.03.024.
[13] K. Szymanska, A.I. Zouboulis, D. Zamboulis, Hybrid ozonation–microfiltration system for the treatment of surface water using ceramic membrane, J. Membr. Sci. 468 (2014) 163–171, http://dx.doi.org/10.1016/j.memsci.2014.05.056.
[14] Bhavana S. Karnik et al., Effects of ozonation on the permeate flux of nanocrystalline ceramic membranes, Water Res. 39 (4) (2005) 728–734, http://dx.doi.org/10.1016/j.watres.2004.11.017.
[15] Urs Von Gunten, Ozonation of drinking water: Part I. Oxidation kinetics and product formation, Water Res. 37 (7) (2003) 1443–1467, http://dx.doi.org/10.1016/S0043-1354(02)00457-8.
[16] Y. Mori et al., Ozone-microfiltration system, Desalination 117 (1) (1998) 211–218, http://dx.doi.org/10.1016/S0011-9164(98)00098-8.
[17] S.H. Davies et al., Fabrication of catalytic ceramic membranes for water filtration, Water Sci. Technol.: Water Supply 10 (1) (2010) 81–86, http://dx.doi.org/10.2166/ws.2010.789.
[18] Bhavana S. Karnik et al., Fabrication of catalytic membranes for the treatment of drinking water using combined ozonation and ultrafiltration, Environ. Sci. Technol. 39 (19) (2005) 7656–7661, http://dx.doi.org/10.1021/es0503938.
[19] Lindsay M. Corneal et al., Mn oxide coated catalytic membranes for hybrid ozonation-membrane filtration: Membrane microstructural characterization, J Membr. Sci. 369 (1) (2011) 182–187, http://dx.doi.org/10.1016/j.memsci.2010.11.071.
[20] Lindsay M. Corneal et al., AFM, SEM and EDS characterization of manganese oxide coated ceramic water filtration membranes, J. Membr. Sci. 360 (1) (2010) 292–302, http://dx.doi.org/10.1016/j.memsci.2010.05.026.
[21] A. Zouboulis, D. Zamboulis, K. Szymanska, Hybrid membrane processes for the treatment of surface water and mitigation of membrane fouling, Sep. Purif. Technol. 137 (2014) 43–52, http://dx.doi.org/10.1016/j.seppur.2014.09.023.
[22] Dequan Wei et al., Effect of pre-ozonation on mitigation of ceramic UF membrane fouling caused by algal extracellular organic matters, Chem. Eng. J. 294 (2016) 157–166, http://dx.doi.org/10.1016/j.cej.2016.02.110.
[23] Dequan Wei et al., Effect of in-situ ozonation on ceramic UF membrane fouling mitigation in algal-rich water treatment, J. Membr. Sci. 498 (2016) 116–124, http://dx.doi.org/10.1016/j.memsci.2015.09.063.
[24] Jeonghwan Kim et al., Effect of ozone dosage and hydrodynamic conditions on the permeate flux in a hybrid ozonation–ceramic ultrafiltration system treating natural waters, J. Membr. Sci. 311 (1) (2008) 165–172, http://dx.doi.org/10.1016/j.memsci.2007.12.010.
[25] A. David, Chin, Fluid Mechanics for Engineers, Pearson Higher Education, Hoboken, NJ, 2015, pp. 614–615.
[26] Rodney J. Allam, Improved oxygen production technologies, Energy Procedia 1 (1) (2009) 461–470, http://dx.doi.org/10.1016/j.egypro.2009.01.062.
[27] Wen-feng Tan et al., Determination of the point-of-zero charge of manganese oxides with different methods including an improved salt titration method, Soil Sci. 173 (4) (2008) 277–286, http://dx.doi.org/10.1097/SS.0b013e31816d1f12.